TMA4180 Optimisation: Form-finding of tensegrity structures

August Rolfsen, Ine Daiwei Zhao, Matias Sunde Øiesvold and Ola Tangen Kulseng

April 2023

1 Abstract

In this paper we show how one can use optimization techniques to find stable tensegrity structures. We do this by finding local minimizers of the mechanical energy of the system. There will be a focus on the theoretical aspects of the structures, but there is a section at the end with numerical results. For numerical optimisation, we applied the BFGS method.

2 Introduction

2.1 Modeling of the structures

Tensegrity structures consist of bars and cables that are connected with joints. We will model the structures as a directed graph $\mathcal{G} = (\mathcal{V}, \mathcal{E})$, where $\mathcal{V} = \{1, ..., N\}$ is a set of vertices, and $\mathcal{E} \subset \mathcal{V} \times \mathcal{V}$ is a set of edges. The vertices naturally represent the joints of the structure, and an edge $e_{ij} = (i, j)$ with $i < j$ indicates that the joints i and j are connected through either a cable or a bar.

The position of a node i is given by $x^{(i)} = (x_1^{(i)}, x_2^{(i)}, x_3^{(i)})$. Additionally, we will collect the position of all nodes in a vector $X = (x^{(1)}, ..., x^{(N)}) \in \mathbb{R}^{3N}$

The goal is to determine the position X of all the nodes. We rely on the physical principle that the structure will assume a stable resting position X^* only when the total potential energy of the system has attained a local minimum. This naturally gives rise to an optimization problem.

We will assume that all bars are made of the same material with identical thickness and cross section. They can, however, have different *rest length*. The rest length of a bar between node i and node j, ℓ_{ij}, is defined to be the positive real number at which the internal elastic energy is 0. If the bar is stretched or compressed to a new length $L(e_{ij}) = \|x^{(i)} - x^{(j)}\|$, we will model the energy using a quadratic model

$$E_{elast}^{bar}(e_{ij}) = \frac{c}{2\ell_{ij}^2}(L(e_{ij}) - \ell_{ij})^2 = \frac{c}{2\ell_{ij}^2}(\|x^{(i)} - x^{(j)}\| - \ell_{ij})^2 \tag{1}$$

where the parameter $c > 0$ depends on the material and cross section of the bar.

We also consider the effects of gravity on the bars, as they may be of considerable mass. Introducing ρ as the line density of all the bars in the system, we will use

$$E_{grav}^{bar}(e_{ij}) = \frac{\rho g \ell_{ij}}{2}(x_3^{(i)} + x_3^{(j)}) \tag{2}$$

where g is the acceleration due to gravity.

Cables are modeled similarly to bars. We will assume them to be massless, and only extendable. They too have a rest length, but the energy function is 0 if the length between the nodes is smaller than the rest length. Thus

$$E_{elast}^{cable}(e_{ij}) = \begin{cases} \frac{k}{2\ell_{ij}^2}(\|x^{(i)} - x^{(j)}\| - \ell_{ij})^2 & \text{if} \quad \|x^{(i)} - x^{(j)}\| > \ell_{ij} \\ 0 & \text{if} \quad \|x^{(i)} - x^{(j)}\| \leq \ell_{ij} \end{cases} \tag{3}$$

where $k > 0$ is a material parameter.

The resulting structures give more physical meaning if we let the nodes be point particles with a finite mass, contributing a value of

$$E_{ext}(X) = \sum_{i=1}^{N} m_i g x_3^{(i)} \tag{4}$$

to the energy. The objective function to be minimized is then the total energy given by the following equation:

$$E(X) = \sum_{e_{ij} \in \mathcal{B}} (E_{elast}^{bar}(e_{ij}) + E_{grav}^{bar}(e_{ij})) + \sum_{e_{ij} \in \mathcal{C}} E_{elast}^{cable}(e_{ij}) + E_{ext}(X) \tag{5}$$

where $\mathcal{B}, \mathcal{C} \subset \mathcal{E}$ are the sets of bars and cables in the structure.

The elastic potential for the cables is a piecewise continuous function. To show that it is everywhere continuous, we need to show that it is also continuous at the branch points. This is, however, straighforward as $L(e_{ij}) - \ell_{ij} \to 0$ when $L(e_{ij}) \to \ell_{ij}$. As (5) then is a sum of continuous functions, we conclude that it is continuous.

Note that minimizing (5) might not admit a solution, as the energy can be unbounded from below by letting all z-coordinates of the nodes tend to $-\infty$. We propose two solutions to this issue.

2.2 Fixing the position of a set of nodes

The first option is fixing some of the nodes such that

$$x^{(i)} = p^{(i)} \qquad \text{for } i = 1, ..., M \tag{6}$$

for some fixed $p^{(i)} \in \mathbb{R}^3$, and $1 \leq M < N$. This constraint is convenient because the resulting problem is an unconstrained one when we can treat the fixed nodes as constants. The dimension of this free optimization problem would then be $3(N - M)$. Constraining just one node will, in fact, theoretically guarantee a solution:

Theorem: If the graph $\mathcal{G}$ is connected, the objective function (5) with the constraint (6) admits a solution, as long as k and c are nonzero

Proof: We have already shown that (5) is continuous and thus lower semi-continuous. It is therefore sufficient to show coercivity.

Let p be a fixed node and let x be any free node. Without loss of generality, we may set $p_1 = p_2 = 0$. As $\mathcal{G}$ is connected, there must exist some set of nodes $\mathcal{S}$ defining a path from x to p.

This path consists of free and or fixed points connected by cables or bars. The key observation is that if the lengths of all the edges in this graph is finite, then the distance between p and x must be finite too. Conversely, this implies that the length of at least one edge must tend to ∞ whenever $\|x - p\| \to \infty$.

Now, both (1) and tend quadratically to $+\infty$ when the norm does. The only term in (5) that can counteract this positive infinity is the negative gravitational potential of the bars and the free weights. Both (2) and (4) are linearly dependent on the x_3 components however, and must therefore be dominated for large values of x_3. □

In a disconnected graph, one would have to fix a node in each connected subgraph. We will not consider these situations in this paper, so we will not prove this.

2.3 Imposing positive z-values of the nodes

The proof of section 2.2 suggest that only gravity may let the total energy function tend to $-\infty$. To support freestanding structures, it is therefore natural to impose the inequality constraints

$$x_3^{(i)} \geq 0 \quad \forall \quad i = 1, ..., N \tag{7}$$

forcing all free points to be above ground.

Note that coerciveness is not as immediate in this case. If we simultaneously move all the nodes horizontally in any direction, we see that the distance between the nodes do not change, and thus the energy is constant. This issue can be solved without a loss of generality by fixing the x_1 and x_2-position of a given node: $x^{(i)} = (p_1, p_2, x_3^{(i)})$. This simply disallows moving the entire structure horizontally.

Theorem: If the graph $\mathcal{G}$ is connected, the objective function (5) with the constraint (7) admits a solution.

With this setup, coerciveness mostly follows from the proof in the theorem above. Note that we do not allow $x_3 \to -\infty$ because of the constraint (7). Additionally, note that the energy from $E_{elast}^{cable}(e_{ij})$ and $E_{elast}^{bar}(e_{ij})$ does not tend to ∞ when we increase z simultaneously for all nodes. However, in this case the external force and bar weight will increase, and thus the total energy function is coercive. □

Note that this restriction indeed creates a constrained optimisation problem, unlike the constraint (6) where we had a free optimization problem in a lower dimension.

3 Cable net structures

In this section, we are analyzing the situation where all members of the structure are cables, and where we fix certain nodes in order to ensure that a solution exists. This gives us the following optimization problem:

$$\min_X E(X) = \sum_{e_{ij} \in \mathcal{E}} E_{elast}^{cable}(e_{ij}) + E_{ext}(X) \quad \text{s.t. } x^{(i)} = p^{(i)}, i = 1, ..., M \tag{8}$$

In order to solve this optimization problem, we first have to show some properties about the function. We have already shown that the more general problem (5) is continuous, therefore (8) is continuous.

3.1 Differentiability

Theorem: The function given in (8) is C^1.

We will consider this function term by term. The gradient of $E_{ext}(X)$ is

$$\nabla E_{\mathbf{ext}}(X) = \nabla \sum_{i=1}^{N} m_i g x_3^{(i)} = (0, 0, m_1 g, 0, 0, m_2 g, ..., 0, 0, m_N g) \tag{9}$$

which is continuous. In fact, it's clear that $E_{ext}(X) \in C^\infty$. The term $E_{elast}^{cable}(e_{ij})$ is obviously differentiable when $\|x^{(i)} - x^{(j)}\| \neq \ell_{ij}$. A trivial calculation yields

$$\lim_{\|x^{(i)} - x^{(j)}\| \to \ell_{ij}^-} \nabla E_{elast}^{cable}(e_{ij}) = 0 \tag{10}$$

If the gradient is to be continuous, one must have

$$\lim_{\|x^{(i)} - x^{(j)}\| \to \ell_{ij}^+} \nabla E_{elast}^{cable}(e_{ij}) = 0 \tag{11}$$

The partial derivatives with respect to $x_s^{(i)}$ where s represents one of the three directions $s = 1, 2, 3$, are given by

$$\frac{\partial}{\partial x_s^{(i)}} E_{elast}^{cable}(e_{ij}) = \frac{\partial}{\partial x_s^{(i)}} \frac{k}{2\ell_{ij}^2} (\|x^{(i)} - x^{(j)}\| - \ell_{ij})^2 = \frac{k}{\ell_{ij}^2} (1 - \frac{\ell_{ij}}{\|x^{(i)} - x^{(j)}\|})(x_s^{(i)} - x_s^{(j)}) \tag{12}$$

The limit as $\|x^{(i)} - x^{(j)}\| \to \ell_{ij}^+$ is clearly 0.

This holds for all partial derivatives, which shows that the function is C^1. Note that $\|x^{(i)} - x^{(j)}\| > \ell_{ij}$, so we never divide by zero. Thus we have a sum of C^1 functions, which is C^1. □

However, the function is not C^2. Again consider the situation when $\|x^{(i)} - x^{(j)}\| > \ell_{ij}$:

$$\frac{\partial}{\partial x_2^{(i)}} \frac{\partial}{\partial x_1^{(i)}} E_{elast}^{cable}(e_{ij}) = \frac{\partial}{\partial x_2^{(i)}} \left(\frac{k}{\ell_{ij}^2} (1 - \frac{\ell_{ij}}{\|x^{(i)} - x^{(j)}\|})(x_1^{(i)} - x_1^{(j)}) \right) = \frac{k}{\ell_{ij}} \frac{(x_1^{(i)} - x_1^{(j)})(x_2^{(i)} - x_2^{(j)})}{\|x^{(i)} - x^{(j)}\|^3}$$

Which we see is not zero in the limit as $\|x^{(i)} - x^{(j)}\| \to \ell_{ij}^+$.

3.2 Convexity

Theorem: The cable net objective function (8) is convex, but not strictly convex

As a sum of convex functions is itself convex, we will again consider the function term by term.

First consider $E_{ext}(X) = \sum_{i=1}^{N} m_i g x_3^{(i)}$. This is convex, but not strictly convex due to linearity.

Next consider $\sum_{e_{ij} \in \mathcal{E}} E_{elast}^{cable}(e_{ij})$. Let $\mu > 0, \kappa > 0$ be constants. Further, let $g : \mathbb{R}^3 \times \mathbb{R}^3 \to \mathbb{R}$ and $f : \mathbb{R} \to \mathbb{R}$ be functions defined by

$$g(x^{(i)}, x^{(j)}) := \kappa f(\|x^{(i)} - x^{(j)}\|) \qquad f(t) := \begin{cases} (t-\mu)^2 & , t > \mu \\ 0 & , t \leq \mu \end{cases}$$

Observing that

$$E_{elast}^{cable}(e_{ij}) = g(x^{(i)}, x^{(j)}) = \kappa f(t)$$

for $t = \|x^{(i)} - x^{(j)}\|, \mu = l_{ij}$ and $\kappa = \frac{k}{2l_{ij}^2}$, it is sufficient to show that f and g is convex. g is a norm, and is therefore known to be convex. Differentiating f, one obtains

$$f'(t) := \begin{cases} 2(t-\mu) & , t > \mu \\ 0 & , t \leq \mu \end{cases}$$

This shows for all $t > \mu$, $f'(t)$ is non-negative and thus the function value increases. Hence, $f(t)$ is a convex function. □

Note that (8) is not strictly convex as neither f nor $E_{ext}(X)$ are strictly convex.

The fact that this energy expression is convex means that Quasi-Newton methods are a good candidate. Newton's method is, of course, not an option, as our function is not C^2,

3.3 Necessary and sufficient optimality conditions

As we have a convex function that is differentiable, the necessary and sufficient optimality condition for a solution X^* is simply

$$\nabla E(X^*) = 0 \tag{13}$$

This will be a global minimizer due to convexity. It will not necessarily be unique, as that would require strict convexity.

4 Tensegrity domes

We will now consider the full optimisation problem (5) subject to the constraints of equation 6.

4.1 Differentiability

Differentiating the objective function (5), one obtains

$$\frac{\partial}{\partial x_s^{(i)}} E_{elast}^{bar}(e_{ij}) = \frac{c}{\ell_{ij}^2}(1 - \frac{\ell_{ij}}{\|x^{(i)} - x^{(j)}\|})(x_s^{(i)} - x_s^{(j)}) \tag{14}$$

which is not defined when the norm is 0 (i.e two points connected by a bar coincide). This could pose a problem numerically if the actual solution to the system contain bars with coinciding endpoints. However, the norm of the gradient remains *finite* when the points approach each other due to the last factor in (14). This helps tremendously when running the numerical routines, as the worst case scenario is the solver bouncing back and forth and not some divide by zero error. By adding some small positive number (close to machine precision), the points would never technically coincide anyway.

One could argue that the original problem in these cases is ill-posed, but it may be difficult to know a priori whether or not it is energetically beneficial to remove a bar for complex structures.

4.2 Convexity

Theorem: The full optimisation problem (5) is not convex.
Consider $\lambda = \frac{1}{2}$, and X, Y such that

$$\|x^{(i)} - x^{(j)}\| = \|y^{(i)} - y^{(j)}\| = \ell_{ij} \quad \forall \quad i, j \in N \tag{15}$$

Now let $Y = -X$, that is: $x^{(i)} - x^{(j)} = -(y^{(i)} - y^{(j)}) = y^{(j)} - y^{(i)}$ such that

$$E(\lambda X + (1-\lambda)Y) = E(\frac{1}{2}X + \frac{1}{2}(-X)) = E(0) = \sum_{e_{ij}\in\mathcal{B}} \frac{c}{2\ell_{ij}^2}(\|0\| - \ell_{ij})^2 = \sum_{e_{ij}\in\mathcal{B}} \frac{c}{2} \tag{16}$$

which is greater than zero as $c > 0$. On the other hand with assumption (15), we get the following result,

$$\begin{aligned} &\lambda E(X) + (1-\lambda)(Y) = \frac{1}{2}E(X) + \frac{1}{2}E(-X) \\ &= \frac{1}{2}\sum_{e_{ij}\in\mathcal{B}} \frac{c}{2\ell_{ij}^2}(\|x^{(i)} - x^{(j)}\| - \ell_{ij})^2 + \frac{1}{2}\sum_{e_{ij}\in\mathcal{B}} \frac{c}{2\ell_{ij}^2}(\|x^{(i)} - x^{(j)}\| - \ell_{ij})^2 = 0 \end{aligned} \tag{17}$$

$$E(\lambda X + (1-\lambda)Y) = \sum_{e_{ij}\in\mathcal{B}} \frac{c}{2} \not\leq 0 = \lambda E(X) + (1-\lambda)E(Y)$$

Thus showing that the objective function is not convex. □

4.3 Optimality conditions for tensegrity domes

For C^2 optimisation problems, the general necessary optimality conditions for a local solution X^* are

$$\begin{aligned} &\nabla E(X^*) = 0 \\ &H_f(X^*) \text{ is positive semi-definite} \end{aligned}$$

However, our objective function is not C^2 so we have no necessary second order conditions. For all practical purposes, we still have the necessary condition $\nabla E(X^*) = 0$. As $E(X)$ is not convex, the neccesary condition $\nabla E(X) = 0$ is not sufficient. However, in this project we are not only interested in the global minimum, as local solutions correspond to stable physical systems.

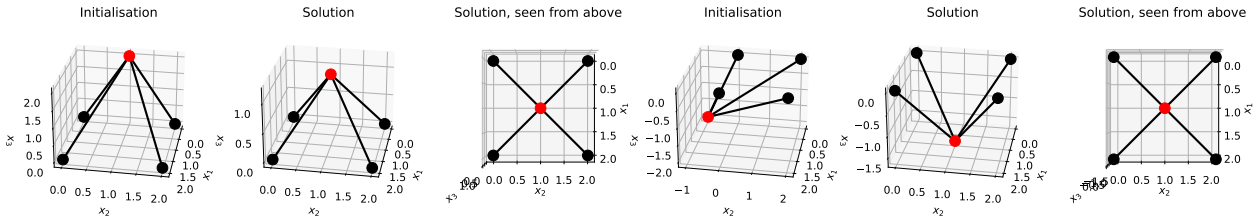

Figure 1: Local optimizer to the left, global optimizer to the right. The free node $x^{(0)}$ placed above the xy-plane and is connected through bars to four fixed nodes. The position of $x^{(0)}$ will be determined by the equilibrium between external load, gravity, and elastic energy of the bar. However, if we initialize the free node below the xy-plane, we will reach a global minima. Notice that the x_1 and y-position is equal, only the z-component differs. Numerics will be discussed later in the paper.

4.4 Local minima

As the function is non-convex, there can exist non-global minima as seen in figure 1. These plots were generated by the numerical algorithm described in later sections. The main takeaway is that two solutions exist to this simple problem, and the algorithm may converge to either depending on the initial conditions.

5 Tensegrity domes in constrained optimization

We will now consider the full problem (5) with the constraints given by (7). As this is a constrained optimization problem, we define the Lagrangian

$$\mathcal{L}(X, \lambda) = E(X) - \sum_{i \in \mathcal{I}} \lambda_i c_i(X) \tag{18}$$

Where $c_i(X) = x_3^{(i)}$. The first order optimality conditions for a given (X^*, λ^*) are

$$\begin{aligned} &\nabla_x \mathcal{L}(X, \lambda^*) = 0 \\ &x_3^{*(i)} \geq 0, \quad \lambda_i^* \geq 0 \quad \lambda_i^* x_3^{*(i)} = 0, \quad i = 1, ..., N \end{aligned} \tag{19}$$

As for LICQ we have

$$\begin{aligned} \nabla c_1(X) = \left(\frac{\partial c_1}{\partial x^{(1)}}, \frac{\partial c_1}{\partial x^{(2)}}, ..., \frac{\partial c_1}{\partial x^{(i)}}, ..., \frac{\partial c_1}{\partial x^{(N)}} \right) &= \Big((0,0,1), (0,0,0), ..., (0,0,0), ..., (0,0,0) \Big) \\ \nabla c_i(X) &= \Big((0,0,0), (0,0,0), ..., \underbrace{(0,0,1)}_{i^{\text{th}} \text{ term}}, ..., (0,0,0) \Big) \\ \nabla c_N(X) &= \Big((0,0,0), (0,0,0), ..., (0,0,0), ..., (0,0,1) \Big) \end{aligned}$$

It's clear that the inequality constraints $\{\nabla c_i(X), i = 1, 2, ..., N\}$ are linearly independent as there are no vectors with non-zero terms in the same dimension. This means LICQ holds, and therefore the KKT conditions are neccesary, but they are not sufficient as our problem is not convex.

5.1 Horizontal translational invariance

Recall that a simultaneous shift of all nodes in any horizontal direction does not impact the total energy. For $E_{elast}^{cable}(e_{ij})$ and $E_{elast}^{bar}(e_{ij})$, this is clear as the norm will be constant. As for $E_{grav}^{bar}(e_{ij})$ and $E_{ext}(X)$, these only depend on vertical shifts. When developing numerical methods, this can cause issues due to the non-uniqueness of solutions. The easiest workaround is to fix nodes, as discussed extensively in section 2.2 and 2.3.

6 Numerical

6.1 Methods

Section 6.2 includes a number of numerical experiments and results. This section explains how we arrived at those results, by showing our programmatic approach to the problem. The code used to solve the optimization problems and to generate the figures can be found in this Github repository.

6.1.1 BFGS

This is a completely generic implementation of the BFGS method in the algoritmer.py file. The implementation follows closely that of algorithm 6.1 in [NW06], the only difference being the choice of steplength. Our implementation uses a line search method to find a steplength that satisfies the *strong* Wolfe conditions, rather than the regular ones used in the book.

The linesearch method is based on algorithm 3.5 in [NW06], with a bisecting interpolation implementation of zoom (algorithm 3.6). The next steplength is chosen according to $\alpha_{k+1} = \gamma\alpha_k$. The number γ together with c_1 and c_2 completely specify the algorithm, and are preset as

γ	c_1	c_2
2	0.01	0.9

The BFGS iterations stop either when some predetermined maximum iterations has been reached, or when the norm of the gradient is below a threshold of 1×10^{-14}.

BFGS has been shown to converge under certain assumptions, most notably convexity and the objective function being twice continiously differentiable. The objective functions we consider in this project are not C^2, and only (8) is convex. One could consider applying other methods such as gradient descent as they have better theoretical guarantees of convergence, but they are significantly slower than BFGS. As BFGS is known to work very well in practice, we will exclusively use this algorithm in this project.

6.1.2 Tensegrity

This is the generation of objective and gradient functions, and can be found in the tensegrity.py file.

When creating a TensegrityStructure, the functions gen_E and gen_grad_E are called with the corresponding cables, bars, free weights, fixed points and rest lengths and returns the objective and gradient functions of the setup according to the equations in the previous sections. The returned functions take as input only the position of the free points, which are the variables to be optimized. This is neat, as it allows us to use any generic optimization algorithm to solve the problem.

6.1.3 Freestanding structures

Instead of solving (5) subject to (7), we added quadratic penalization to the energy and gradient functions. The objective function thus gained a term of the from

$$E_{qp} = \sum_{i \in \mathcal{N}} \frac{1}{2}\mu(x_3^{(i)})^2 \tag{20}$$

where $\mathcal{N}$ is the set of all points with z-component smaller than zero. This μ should be large enough to counteract the gravitational pull on the nodes. To avoid having to modify the BFGS method to account for quadratic penalty, we ran BFGS multiple times for increasing values of μ like in the code snippet below.

```
prev = x0
for _ in range(Max_iter):
```

```
res, num = bfgs(prev, ts.func(mu), ts.grad(mu), Niter=1000)
mu *= 1.5
if num < 1000:
    mu *= 2
if num < 500:
    mu *= 2
if num < 250:
    mu *= 2

mu = min(mu, 1e10)
if np.linalg.norm(res - prev) < 1e-12:
    break
prev = res.copy()
```

The code snippet above was used for all freestanding structures.

Freestanding structures may be shifted along any vector in the x_1 - x_2 plane without change in energy, as shown in section 5.1. The structure may also be rotated around any axis parallel to the x_3-axis. These observations affected our convergence. We therefore put three extra constraints on 5:

$$x_1^{(1)} = x_2^{(1)} = 0 \textbf{ and } x_1^{(1)} = x_1^{(2)} \tag{21}$$

The first two constraints fix the position of the structure so that one point ends up close to $(0, 0, 0)$. The last one fixes the orientation of the structure, by requiring that two neigboring points share the same x_1 value. We should only do this with structures having at least two points on the ground. Both of these were added as a quadratic penalty using the same μ as in (20)

6.2 Experiments

The setup for all numerical experiments may be found in the tests.py file. The Tensegrity structure setup is also for convenience given below, before every experiment.

To generate the convergence plots, we compared the intermediate solutions with the correct one. If the solution was unknown, we ran the BFGS routine twice and treated the first iterates solution as the 'analytical' one.

6.2.1 Cable nets

For the first experiment we consider 4 free and 4 fixed nodes along with the following parameters:

$$\text{4 fixed nodes } p^{(1)} = (5, 5, 0),\ p^{(2)} = (-5, 5, 0),\ p^{(3)} = (-5, -5, 0),\ p^{(4)} = (5, -5, 0)$$
$$\text{Cables: } \ell_{15} = \ell_{26} = \ell_{37} = \ell_{48} = \ell_{56} = \ell_{67} = \ell_{78} = \ell_{85} = 3$$
$$k = 3, \quad m_i g = \frac{1}{6}, \quad i = 5, 6, 7, 8$$

This problem has an analytical solution which is given in table (2) along with the numerically obtained solution. We see from figure 3 that we indeed reach this configuration of nodes. We see from the convergence plot that the error norm never increases, presumably a consequence of the function being convex.

6.2.2 Tensegrity domes

We now consider bars as well. The objective function is no longer convex. As discussed previously, $E(X)$ is technically not C^1, but as long as we do not initialize free nodes in the same position, it

Figure 2: Comparison of numerical and analytical solution for the cable net.

Node	Numerical solution	Analytical solution
$x^{(5)}$	$(2, 2, -1.5)$	$(2, 2, -1.5)$
$x^{(6)}$	$(-2, 2, -1.5)$	$(-2, 2, -1.5)$
$x^{(7)}$	$(-2, -2, -1.5)$	$(-2, -2, -1.5)$
$x^{(8)}$	$(2, -2, -1.5)$	$(2, -2, -1.5)$

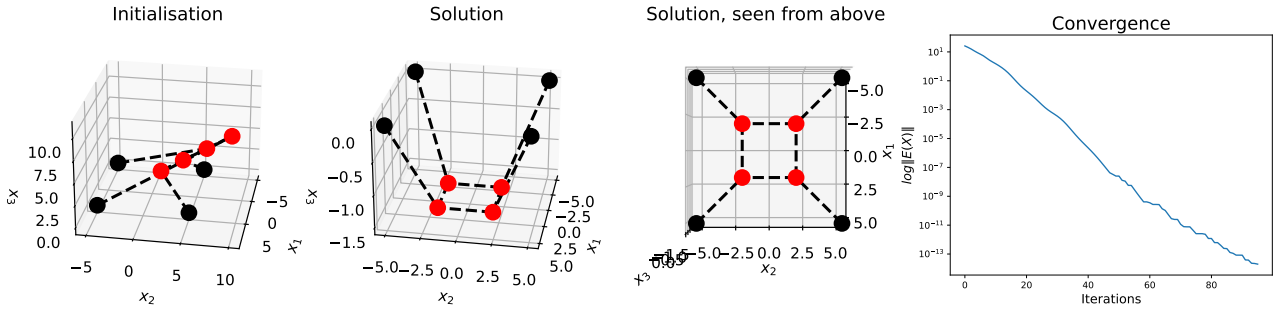

Figure 3: Cable net. Left: Initial node placement. Centre left: Solution. Centre right: Solution from a different viewpoint. Right: Convergence plot using analytical solution.

will be fine in practice. We will test our algorithm with 4 fixed nodes and the following parameters:

$$p^{(1)} = (1, 1, 0),\ p^{(2)} = (-1, 1, 0),\ p^{(3)} = (-1, -1, 0),\ p^{(4)} = (1, -1, 0)$$
$$\text{Cables: } \ell_{18} = \ell_{25} = \ell_{36} = \ell_{47} = 8 \quad \text{and} \quad \ell_{56} = \ell_{67} = \ell_{78} = \ell_{58} = 1$$
$$\text{Bars: } \ell_{15} = \ell_{26} = \ell_{37} = \ell_{48} = 10$$
$$c = 1, \quad k = 0.1, \quad g\rho = 0, \quad m_i g = 0, \quad i = 5, 6, 7, 8$$

We have an analytical solution to this problem, a comparison is given in table 4. We see from figure (5) that we reach the desired configuration of nodes from our initial node placement.

As for the free standing structure, we will consider a configuration fairly close to the Tensegrity dome in order to verify the results. We use the same parameters, but in addition we add the cables $\ell_{12} = \ell_{23} = \ell_{34} = \ell_{41} = 2$ and use a small positive value of $g\rho = 10^{-10}$. We see in figure (6) that we indeed obtain a solution very similar to the tensegrity dome.

As a final experiment, we stack two domes on top of eachother in 7. Note that the convergence plot in this particular case is measuring the norm of the gradient, and not the comparison between some analytic or approximately analytic function evaluation.

Figure 4: Comparison of numerical and analytical solution for the cable net

Node	Numerical solution	Analytical solution
$x^{(5)}$	$(0.70971, 2.30372 \cdot 10^{-8}, 9.54287)$	$(-0.70970, 0, 9.54287)$
$x^{(6)}$	$(6.70558 \cdot 10^{-9}, -0.70971, 9.54287)$	$(0, -0.70970, 9.54287)$
$x^{(7)}$	$(0.70970, 2.98982 \cdot 10^{-8}, 9.54287)$	$(0.70970, 0, 9.54287)$
$x^{(8)}$	$(5.14925 \cdot 10^{-10}, 0.70970, 9.54287)$	$(0, 0.70970, 9.54287)$

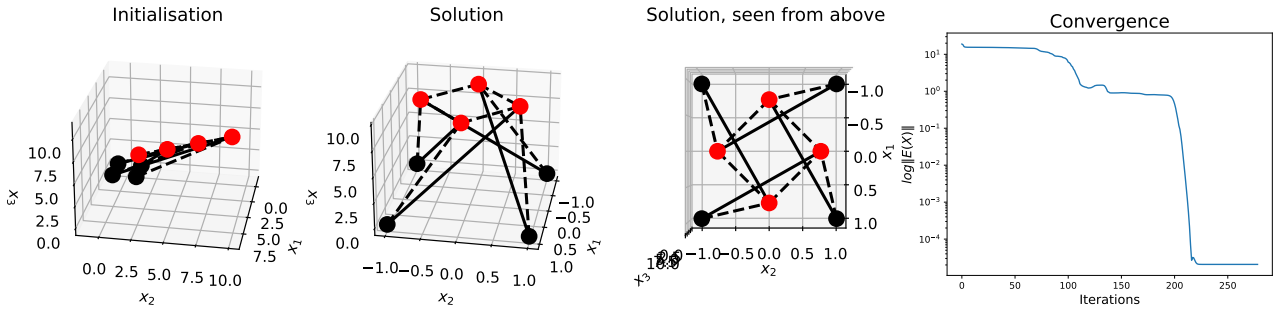

Figure 5: Tensegrity dome. Left: Initial node placement. Centre left: Solution. Centre right: Solution from a different viewpoint. Right: Convergence plot using analytical solution.

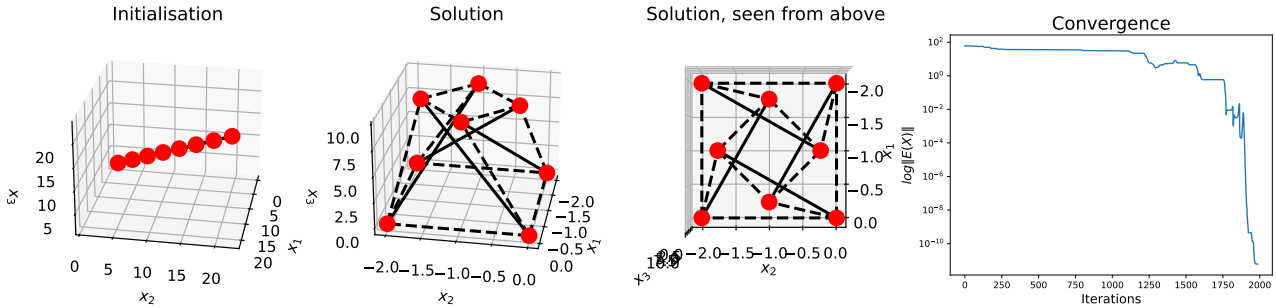

Figure 6: Free standing tensegrity dome. Left: Initial node placement. Centre left: Solution. Centre right: Solution from a different viewpoint. Right: Convergence plot using approximate solution.

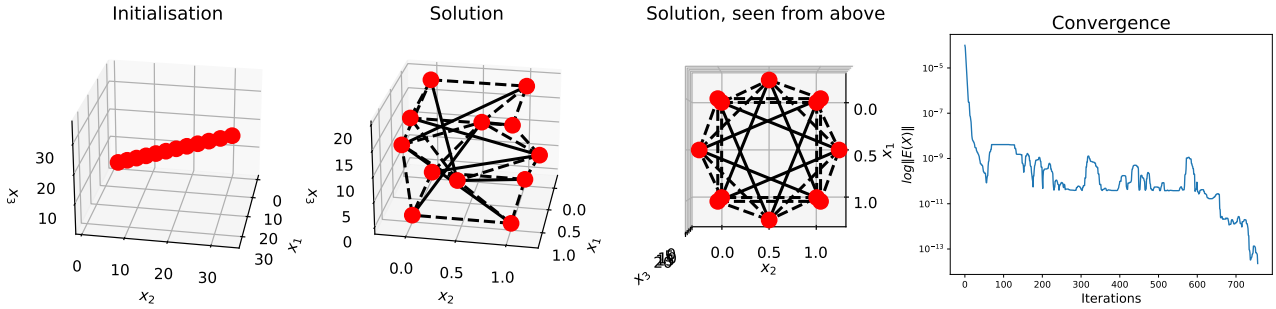

Figure 7: Two free standing tensegrity domes stacked on top of eachothers. Left: Initial node placement. Centre left: Solution. Centre right: Solution from a different viewpoint. Right: Convergence plot using gradient.

7 Conclusion

The numerical results obtained here are only based on the assumption that physical structures assume stationary values of their mechanical energy. Using simple models for bars and cables, this simple insight led to interesting and unconventional structures.

Despite having no theoretical guarantee of convergence, BFGS still managed to find the solutions given in reasonable time. This was not very surprising, given the immense popularity of BFGS.

References

[NW06] Jorge Nocedal and Stephen J. Wright. *Numerical Optimization*. Second. Springer, 2006. ISBN: 0387303030.